1. Supplementary Figure 1 Impact of continuous EES on the threshold to detection of passive movement test performance.
   Scatter plots reporting the detection angle and and plots reporting the error rate (percentage correct trials ± 95% CI) on the TTDPM test performance without EES and when delivering continuous EES at 0.8 and 1.5 times motor response threshold amplitudes and a range of EES frequencies. Different EES frequencies were tested on subject #1 (10 Hz, 50 Hz, 100 Hz) and subject #3 (30 Hz, 50 Hz). At 1.5 motor response threshold amplitude, EES frequencies below 50 Hz induced spasms in the muscles and were thus not tested. Grey dots report the detection angle for successful trials, while pink dots and red crosses indicate false positive and failure to detect movement within the allowed range of motion, respectively (n = 65 for subject #1 and n = 66 for subject #3). *, $P < 0.05$, Clopper-Pearson non-overlapping intervals, two-sided.
2. Supplementary Figure 2 Effect of EES on the natural modulation of proprioceptive circuits during passive movements: extended data.
   a, Configuration of the experimental setup for subject #1 and #3, as described in Fig. 3a. **b**, Plots showing EES pulses, EMG activity of the vastus medialis, and changes in knee joint angle during passive oscillations of the knee when EES is delivered at 60 Hz in subject #2 — similar results were achieved in subject #1 and #3. Conventions as in Fig. 3b.
3. Supplementary Figure 3 Impact of EES amplitude on muscle activity and leg kinematics during locomotion on a treadmill: Subject #1.
   a, AIS leg motor score. **b**, Configuration of electrodes targeting the left and right posterior roots projecting to the L1 and L4 segments. Continuous EES was delivered through these electrodes to facilitate locomotion. **c**, EMG activity of flexor (semitendinosus/tibialis anterior) and extensor (rectus femoris/soleus) muscles spanning the right knee and ankle joints, together with the changes in the knee ankle and foot height trajectories over four gait cycles without EES and with EES delivered at 0.9, 1.2 and 1.5 motor response threshold amplitude — similar results were obtained for 30 gait cycles (analyzed in **d**). EES frequency was set to 40Hz. **d**, Violin plots reporting the root mean square activity of the recorded muscles, the range of motion of the knee and ankle angles, and the step height for different gait cycles (n = 53 gait cycles). Small grey dots represent the different data points, while the large white dots represent the median of the different distributions. Box and whiskers report the interquartile range and the adjacent values, respectively. *, $P < 0.05$, ***, $P < 0.001$, Wilcoxon rank-sum two-sided test with Bonferroni correction for multiple comparisons.
4. Supplementary Figure 4 Impact of EES frequency and amplitude on muscle activity and leg kinematics during locomotion on a treadmill: Subject #2.
   The results displayed in Fig. 6 and Supplementary Figure 3 for subject #1 are reported for subject #2 using the same conventions. Recordings in panels **a** and **c** were repeated for 29 and 20 gait cycles and analyzed in panels **b** and **c**, respectively. The statistics in panel **d** were computed over n = 37 gait cycles. *, $P < 0.05$, ***, $P < 0.001$, Wilcoxon rank-sum two-sided test with Bonferroni correction for multiple comparisons.

5. Supplementary Figure 5 Impact of EES frequency and amplitude on muscle activity and leg kinematics during locomotion on a treadmill: Subject #3.
The results displayed in Fig. 6 and Supplementary Figure 3 for subject #1 are reported for subject #3 using the same conventions. Recordings in panels **a** and **c** were repeated for 51 and 25 gait cycles and were analyzed in panels **b** and **c**, respectively. The statistics in panel **b** and **d** were computed over n = 77 and n = 51 gait cycles, respectively. *, $P < 0.05$, ***, $P < 0.001$, Wilcoxon rank-sum two-sided test with Bonferroni correction for multiple comparisons.
6. Supplementary Figure 6 High-frequency, low-amplitude EES protocols preserve proprioceptive information and promote motor patterns formation.
Impact of continuous high-frequency low-amplitude EES protocols (600 Hz, 20% recruited afferents) on the modulation of the muscle spindle feedback circuits, following the same conventions as in Fig. 5. For comparison, the impact of continuous EES on the group-Ia afferent firings is also reported.
7. Supplementary Figure 7 Integrate-and-fire motor neuron model.
Schematic of the integrate and fire model and of the different synapses contacting this cell. **b**, Simulated inhibitory and excitatory post synaptic potentials (IPSPs/EPSPs) induced by the activation of a single Ia-inhibitory interneuron or a single group-Ia afferent fiber, respectively. **c**, Excitation threshold of our multicompartmental alpha motoneuron model. **d**, Number and amplitude of experimental and modeled EPSP/IPSPs induced from the synaptic contacts originating from group-Ia afferents (s1), group-II excitatory interneurons (s2), and Ia-inhibitory interneurons (s3).
8. Supplementary Figure 8 Adaptation of the rat neural network to humans.
a, Model layout of the hybrid rat-human computational model used to tune the human neural network weights. W_1, w_2, w_3 and w_4 represent the weights of the neural network connections that have been modified to adapt the rat neural network to the human one. **b**, Systematic search results. W_1 and w_3 were ranged together between 1 and 2 times the weight used in the rat network, while w_2 and w_4 were ranged between 1 and 4 times. Bar plots report the percentage of simulations that fulfilled the defined fitness criteria. Selected weights that have been used for further simulations are highlighted with an arrow. **c**, Effect of EES on the natural activity of Ia-inhibitory interneurons and on the production of motor patterns during locomotion, in the hybrid rat-human model for the selected set of synaptic weights. Panels on the left report the average firing rate profiles of the Ia-inhibitory interneuron populations associated to either the flexor or the extensor network, as well as their modulation depth (mean ± SEM, n = 11 gait cycles). Similarly, right-most panels represent the average firing rate profiles of motoneurons and their mean firing rate activity during the phase in which they are active (mean ± SEM, n = 11 gait cycles). Effects of different EES frequencies and amplitudes are reported on the top and bottom panels, respectively.

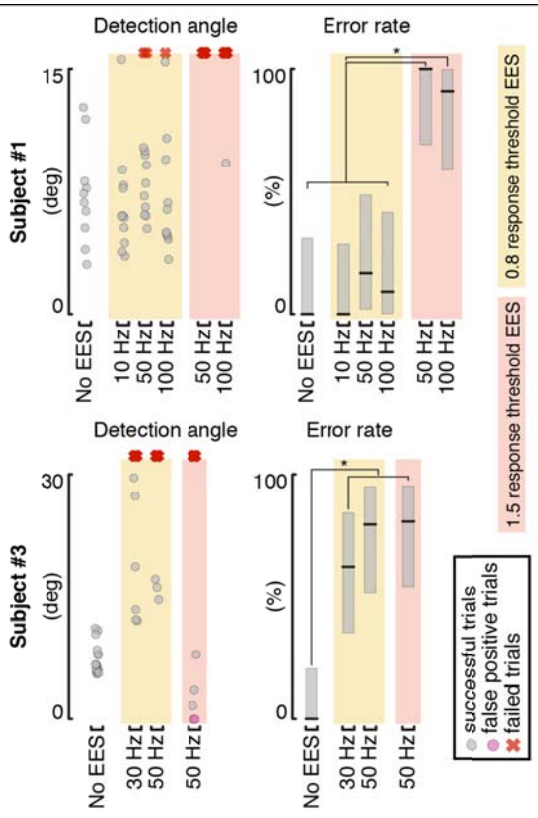

Supplementary Figure 1

Impact of continuous EES on the threshold to detection of passive movement test performance.

Scatter plots reporting the detection angle and and plots reporting the error rate (percentage correct trials ± 95% CI) on the TTDPM test performance without EES and when delivering continuous EES at 0.8 and 1.5 times motor response threshold amplitudes and a range of EES frequencies. Different EES frequencies were tested on subject #1 (10 Hz, 50 Hz, 100 Hz) and subject #3 (30 Hz, 50 Hz). At 1.5 motor response threshold amplitude, EES frequencies below 50 Hz induced spasms in the muscles and were thus not tested. Grey dots report the detection angle for successful trials, while pink dots and red crosses indicate false positive and failure to detect movement within the allowed range of motion, respectively (n = 65 for subject #1 and n = 66 for subject #3). *, P < 0.05, Clopper-Pearson non-overlapping intervals, tow-sided.

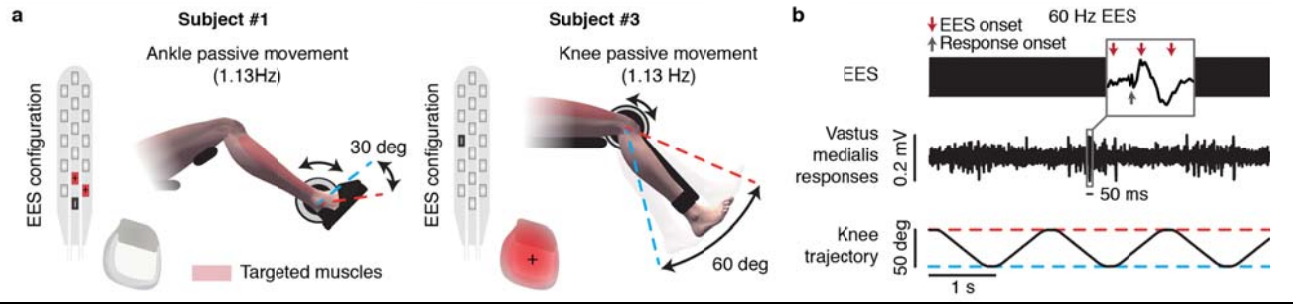

Supplementary Figure 2

Effect of EES on the natural modulation of proprioceptive circuits during passive movements — extended data.

a, Configuration of the experimental setup for subject #1 and #3, as described in **Figure 3a. b,** Plots showing EES pulses, EMG activity of the vastus medialis, and changes in knee joint angle during passive oscillations of the knee when EES is delivered at 60 Hz in subject #2 — similar results were achieved in subject #1 and #3. Conventions as in **Figure 3b.**

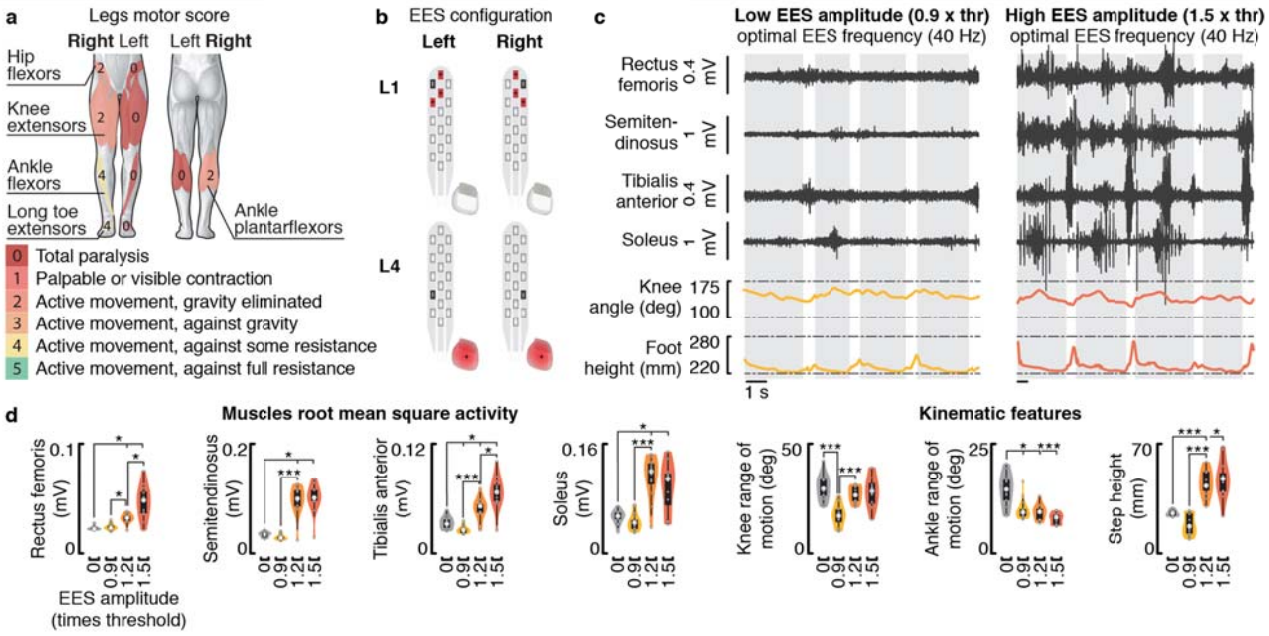

Supplementary Figure 3

Impact of EES amplitude on muscle activity and leg kinematics during locomotion on a treadmill — Subject #1.

a, AIS leg motor score. **b**, Configuration of electrodes targeting the left and right posterior roots projecting to the L1 and L4 segments. Continuous EES was delivered through these electrodes to facilitate locomotion. **c**, EMG activity of flexor (semitendinosus/tibialis anterior) and extensor (rectus femoris/soleus) muscles spanning the right knee and ankle joints, together with the changes in the knee ankle and foot height trajectories over four gait cycles without EES and with EES delivered at 0.9, 1.2 and 1.5 motor response threshold amplitude — similar results were obtained for 30 gait cycles (analyzed in **d**). EES frequency was set to 40Hz. **d**, Violin plots reporting the root mean square activity of the recorded muscles, the range of motion of the knee and ankle angles, and the step height for different gait cycles (n = 53 gait cycles). Small grey dots represent the different data points, while the large white dots represent the median of the different distributions. Box and whiskers report the interquartile range and the adjacent values, respectively. *, $P < 0.05$, ***, $P < 0.001$, Wilcoxon rank-sum two-sided test with Bonferroni correction for multiple comparisons.

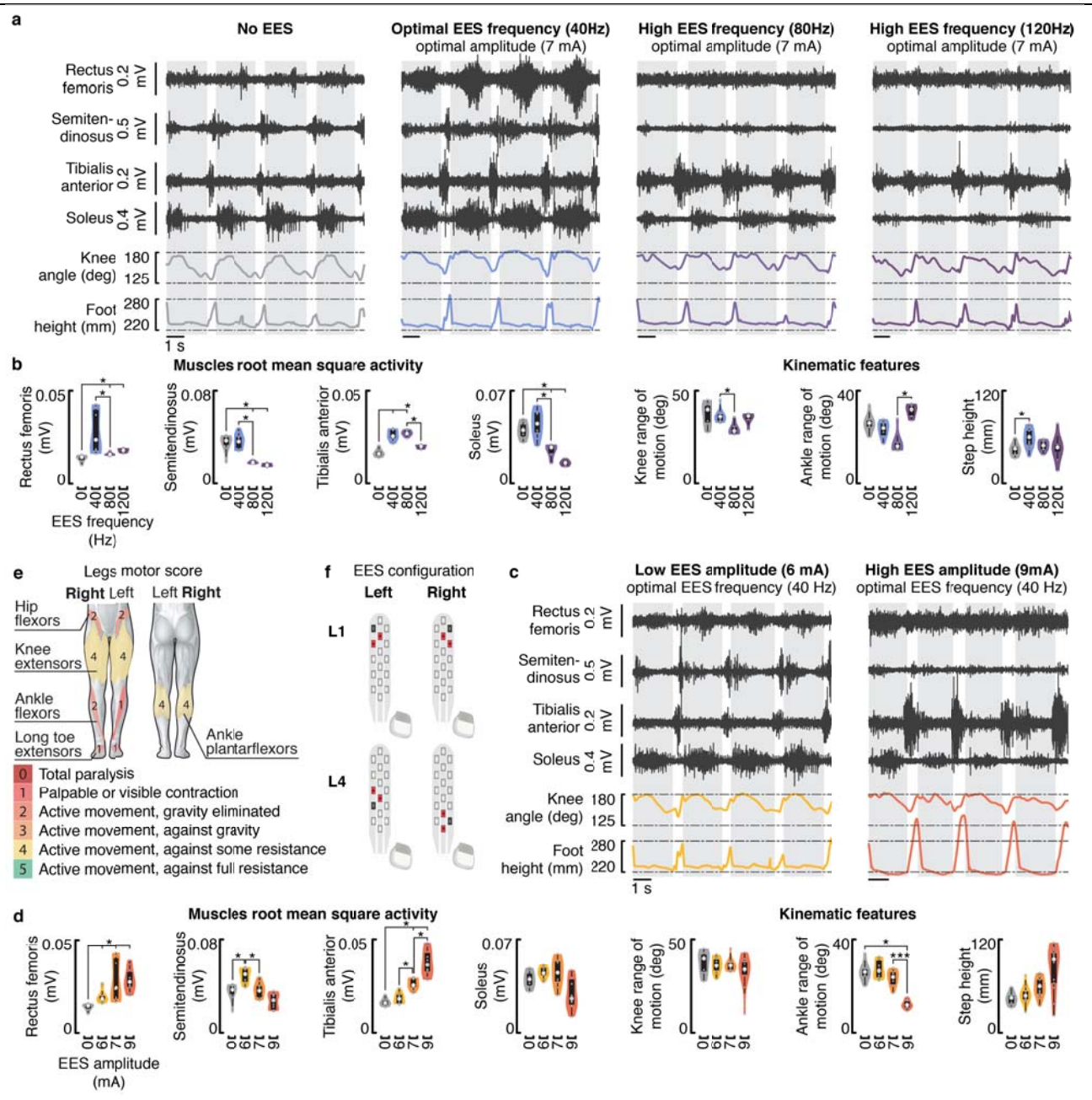

Supplementary Figure 4

Impact of EES frequency and amplitude on muscle activity and leg kinematics during locomotion on a treadmill — Subject #2.

The results displayed in **Figure 6** and **Supplementary Figure 3** for subject #1 are reported for subject #2 using the same conventions. Recordings in panels **a** and **c** were repeated for 29 and 20 gait cycles and analyzed in panels **b** and **c**, respectively. The statistics in panel **d** were computed over n = 37 gait cycles. *, $P < 0.05$, ***, $P < 0.001$, Wilcoxon rank-sum two-sided test with Bonferroni correction for multiple comparisons.

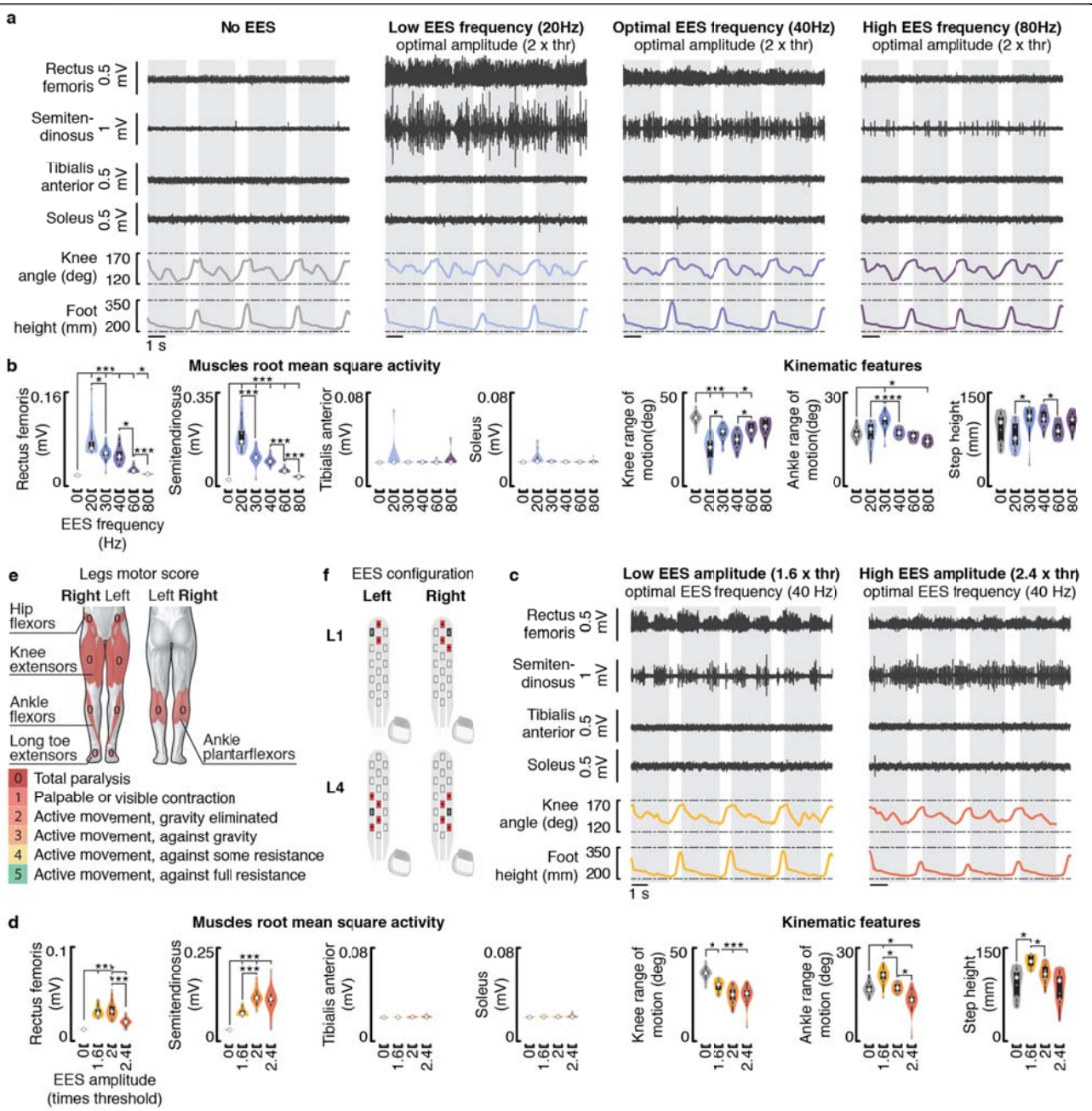

Supplementary Figure 5

Impact of EES frequency and amplitude on muscle activity and leg kinematics during locomotion on a treadmill — Subject #3.

The results displayed in **Figure 6** and **Supplementary Figure 3** for subject #1 are reported for subject #3 using the same conventions. Recordings in panels **a** and **c** were repeated for 51 and 25 gait cycles and were analyzed in panels **b** and **c**, respectively. The statistics in panel **b** and **d** were computed over n = 77 and n = 51 gait cycles, respectively. *, $P < 0.05$, ***, $P < 0.001$, Wilcoxon rank-sum two-sided test with Bonferroni correction for multiple comparisons.

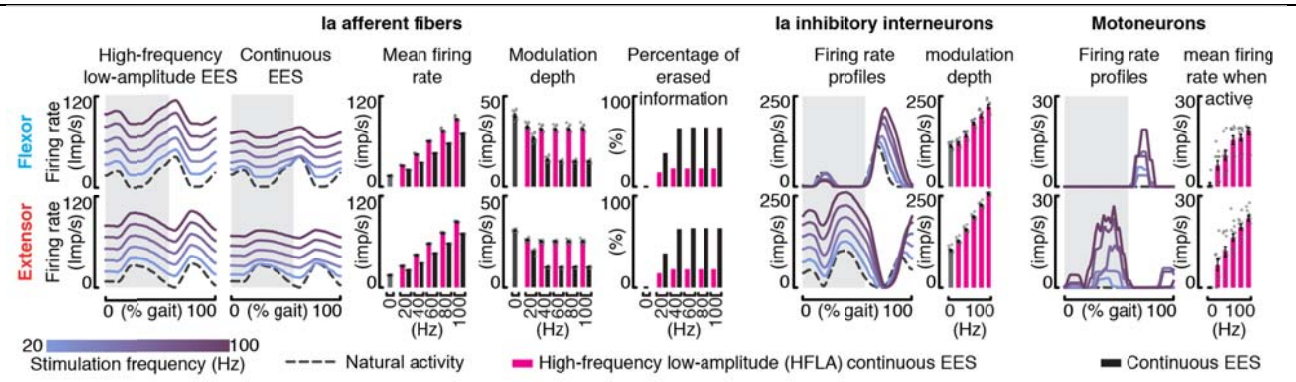

Supplementary Figure 6

High-frequency low-amplitude EES protocols preserve proprioceptive information and promote motor patterns formation.

Impact of continuous high-frequency low-amplitude EES protocols (600 Hz, 20% recruited afferents) on the modulation of the muscle spindle feedback circuits, following the same conventions as in **Figure 5**. For comparison, the impact of continuous EES on the group-Ia afferent firings is also reported.

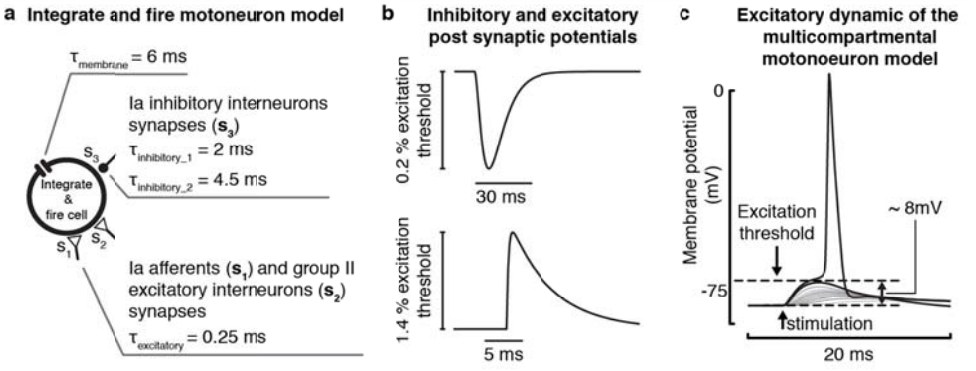

d

	s_1	s_2	s_3
Number of synapses	60	116	232
Experimental IPSP/EPSP	52 / 212 μV	~ 0.33·s_1 EPSP	~ -0.13 μV
Integrate and fire IPSP/EPSP	1.4% excitation threshold	0.7% excitation threshold	-0.2% excitation threshold

Supplementary Figure 7

Integrate and fire motoneuron model.

Schematic of the integrate and fire model and of the different synapses contacting this cell. **b,** Simulated inhibitory and excitatory post synaptic potentials (IPSPs/EPSPs) induced by the activation of a single Ia-inhibitory interneuron or a single group-Ia afferent fiber, respectively. **c**, Excitation threshold of our multicompartmental alpha motoneuron model. **d**, Number and amplitude of experimental and modeled EPSP/IPSPs induced from the synaptic contacts originating from group-Ia afferents (s1), group-II excitatory interneurons (s2), and Ia-inhibitory interneurons (s3).

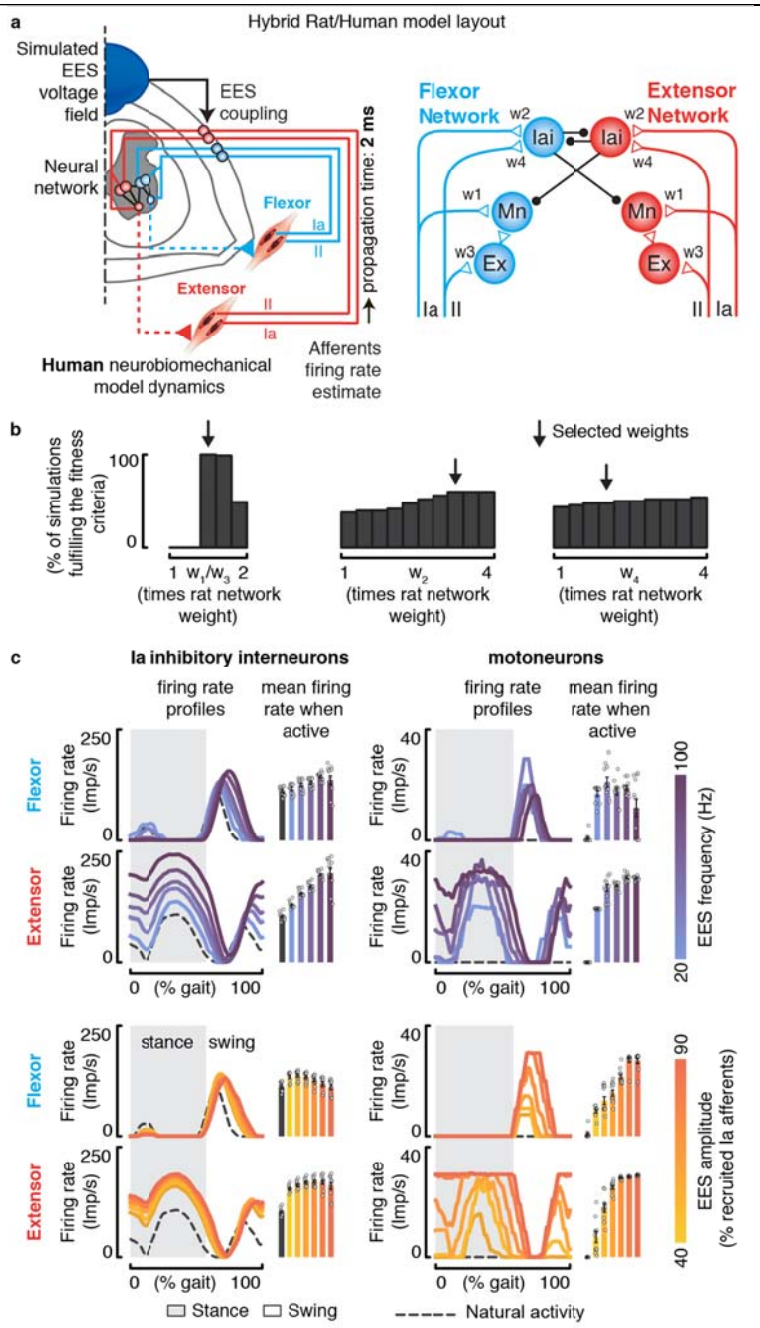

Supplementary Figure 8

Adaptation of the rat neural network to humans.

a, Model layout of the hybrid rat-human computational model used to tune the human neural network weights. W_1, w_2, w_3 and w_4 represent the weights of the neural network connections that have been modified to adapt the rat neural network to the human one. **b**, Systematic search results. W_1 and w_3 were ranged together between 1 and 2 times the weight used in the rat network, while w_2 and w_4 were ranged between 1 and 4 times. Bar plots report the percentage of simulations that fulfilled the

defined fitness criteria. Selected weights that have been used for further simulations are highlighted with an arrow. **c**, Effect of EES on the natural activity of Ia-inhibitory interneurons and on the production of motor patterns during locomotion, in the hybrid rat-human model for the selected set of synaptic weights. Panels on the left report the average firing rate profiles of the Ia-inhibitory interneuron populations associated to either the flexor or the extensor network, as well as their modulation depth (mean ± SEM, n = 11 gait cycles). Similarly, right-most panels represent the average firing rate profiles of motoneurons and their mean firing rate activity during the phase in which they are active (mean ± SEM, n = 11 gait cycles). Effects of different EES frequencies and amplitudes are reported on the top and bottom panels, respectively.

#

Subject	#1	#2	#3
Gender	m	m	m
Age (y)	28	35	47
Years after SCI	6	6	4
WISCI II score	13	6	0
AIS	C	D	C*
Neurological level of injury	C7	C4	C7
UEMS total (max 50)	46	31	45
LER motor subscore (max 25)	14	13	0
LEL motor subscore (max 25)	0	12	0
LE motor score L2 (R/L)	2/0	2/2	0/0
LE motor score L3 (R/L)	2/0	4/4	0/0
LE motor score L4 (R/L)	4/0	2/1	0/0
LE motor score L5 (R/L)	4/0	1/1	0/0
LE motor score S1 (R/L)	2/0	4/4	0/0
LTR sensory subscore	38	29	26
LTL sensory subscore	37	36	29
LE sensory score L1 (R/L)	1/1	1/1	0/0
LE sensory score L2 (R/L)	1/1	1/1	0/0
LE sensory score L3 (R/L)	1/1	1/1	0/1
LE sensory score L4 (R/L)	1/1	1/2	0/0
LE sensory score L5 (R/L)	1/1	1/1	0/1
LE sensory score S1 (R/L)	1/1	0/1	1/1
LE sensory score S2 (R/L)	1/1	0/1	0/1
PPR sensory subscore	17	29	13
PPL sensory subscore	16	36	15
PPR, dermatome L1-S2	0	4	0
PPL, dermatome L1-S2	0	8	0

AIS, American Spinal Injury Association Impairment Scale; LEMS, Lower extremity motor score; SCI, spinal cord injury; LEL, Lower extremity left; LER, lower extremity right; LTL, Light touch left; LTR, Light touch right; PPL, Pin prick left; PPR, Pin prick right; R/L, right/left; UEMS, Upper extremity motor score; WISCI, Walking index for spinal cord injury.

*Reason of AIS C classification in spite of motor scores of 0 throughout all lower extremity key muscles is the presence of voluntary anal contraction.

Supplementary Table 1 | **Subjects' data and neurological status according to the International Standards for Neurological Classification of Spinal Cord Injury.** All the values were collected before the surgical implantation.